

The effects of probabilistic context inference on motor adaptation

Cuevas Rivera, Darío^{1,2} and Kiebel, Stefan J.^{1,2}

¹Chair of Neuroimaging, Faculty of Psychology, Technische Universität Dresden, 01062 Dresden, Germany.
²Centre for Tactile Internet with Human-in-the-Loop (CeTI)

8 Humans have been shown to adapt their movements when a sudden or gradual change
9 to the dynamics of the environment are introduced, a phenomenon called motor adapta-
10 tion. If the change is reverted, the adaptation is also quickly reverted. Humans are also
11 able to adapt to multiple changes in dynamics presented separately, and to be able to
12 switch between adapted movements on the fly. Such switching relies on contextual infor-
13 mation which is often noisy or misleading, affecting the switch between known adaptations.
14 Recently, computational models for motor adaptation and context inference have been in-
15 troduced, which contain components for context inference and Bayesian motor adaptation.
16 These models were used to show the effects of context inference on learning rates across
17 different experiments. We expanded on these works by using a simplified version of the
18 recently-introduced COIN model to show that the effects of context inference on motor
19 adaptation and control go even further than previously shown. Here, we used this model
20 to simulate classical motor adaptation experiments from previous works and showed that
21 context inference, and how it is affected by the presence and reliability of feedback, effect a
22 host of behavioral phenomena that had so far required multiple hypothesized mechanisms,
23 lacking a unified explanation. Concretely, we show that the reliability of direct contextual
24 information, as well as noisy sensory feedback, typical of many experiments, effect measur-
25 able changes in switching-task behavior, as well as in action selection, that stem directly
26 from probabilistic context inference.

Introduction

It has been shown that humans can adapt motor commands to counteract changes in the dynamics of the environment and their own bodies, such as performing reaching movements with a weight attached to the wrist. This is known as motor adaptation. Moreover, human participants have been shown to adapt to different, even opposing, changes during the course of a single experiment (Gandolfo, Mussa-Ivaldi, & Bizzi, 1996; Shadmehr & Brashers-Krug, 1997). Additionally, humans have been shown to dynamically switch between different

34 learned adaptations (Davidson & Wolpert, 2004; Ethier, Zee, & Shadmehr, 2008; Lee &
35 Schweighofer, 2009).

36 By introducing blocks of trials in which body dynamics are altered (e.g. a mechanical
37 arm exerts a force on the participant's hand), experimenters are able to observe motor
38 adaptation through the lens of motor error. Across many different motor adaptation exper-
39 iments (e.g. Davidson & Wolpert, 2004; Gandolfo et al., 1996; Shadmehr & Mussa-Ivaldi,
40 1994), well-established phenomena have been observed: (i) the ability to recall previously-
41 learned skills upon re-exposure to a previous altered dynamic, called savings; (ii) the ability
42 to return to unmodified dynamics, termed de-adaptation; (iii) the interference in motor
43 learning between opposing manipulations in dynamics, called anterograde interference; (iv)
44 spontaneous display of behavior consistent with a previously-learned adaptation, during
45 trials where errors are forced to be zero, called spontaneous recovery.

46 To explain these phenomena, a number of computational models have been introduced,
47 in which motor commands are adapted based on observed motor errors. The most well-
48 studied models are linear learners (Forano & Franklin, 2020; Scheidt, Dingwell, & Mussa-
49 Ivaldi, 2001; Smith, Ghazizadeh, & Shadmehr, 2006), while Bayesian accounts have also
50 been shown to provide an alternative explanation for savings and quick de-adaptation in the
51 form of switching between forward models (Kording & Wolpert, 2004; Oh & Schweighofer,
52 2019).

53 While these general models of adaptation explain the most common phenomena observed
54 in experiments, other known phenomena remain outside of their scope. For example, it is
55 known that adaptation rate is reduced in situations where the environment is unstable and
56 unpredictable (Herzfeld, Vaswani, Marko, & Shadmehr, 2014), or situations in which errors
57 are small (Marko, Haith, Harran, & Shadmehr, 2012) or adaptations slowly introduced
58 (Huang & Shadmehr, 2009). Action selection has also been found to depend on the history
59 of adaptations learned (Davidson & Wolpert, 2004; Vaswani & Shadmehr, 2013).

60 Recently, a new computational model for context-dependant motor learning based on
61 Bayesian inference was introduced by Heald, Lengyel, and Wolpert (2021), called COIN
62 (for context inference). Heald et al. (2021) formalized context inference as a process that
63 operates independently from motor learning, but both informs and is informed by it. With
64 this model, Heald et al. (2021) showed that context inference causes the observed changes
65 in the rate of motor learning in previous experiments (e.g. Herzfeld, Kojima, Soetedjo, &
66 Shadmehr, 2018).

67 In this work we show that the process of context inference underlies more behavioral
68 phenomena than previously shown. We believe that these phenomena stem directly from
69 the process of active inference and the uncertainty that comes with it in a Bayesian setting,
70 as done by Heald et al. (2021), and not from the specific of the generative model used. To
71 show how this Bayesian approach accounts for these phenomena, we used a minimal model
72 for motor adaptation that includes context inference, which we derived by simplifying the
73 COIN model (henceforth called sCOIN). We focused on the effects of uncertain contextual
74 information on switching behavior, especially during error-clamp trials, in which errors are

75 forced to zero by experimenters. More specifically, we focused on the effects of perceptual
76 noise, as well as feedback modalities, in context inference, which in turn affects behavior
77 in ways that can be directly measured. We show that through context inference, switching
78 behavior can display three main effects that have been previously attributed to hypothesized
79 ad-hoc mechanisms: (1) The size of an adaptation dictates how quick and reliable switching
80 between tasks is (Kim, Ogawa, Lv, Schweighofer, & Imamizu, 2015; Oh & Schweighofer,
81 2019), which we explain in terms of the effects of perceptual noise on context inference. (2)
82 Previously-learned adaptations can interfere with switching behavior (Davidson & Wolpert,
83 2004), which we explain in terms of uncertain context inference. (3) Training history (i.e.
84 which adaptations have been learned and for how long) affects switching during error-clamp
85 trials (Vaswani & Shadmehr, 2013), which we also attribute to uncertain context inference.
86 To do this, we used the sCOIN model to simulate the experimental setups and the decision-
87 making agents (i.e. participants) during those experiments.

88 Importantly, the goal of this work is not to introduce a new model for contextual motor
89 learning, but to use the existing ideas of the COIN model to show that context inference
90 can explain more experimental phenomena than those explored by Heald et al. (2021).

91 With these combined simulations and the qualitative comparison to the experimental
92 phenomena outlined above, we provide further evidence that context inference is a sin-
93 gle, coherent and mechanistic account that underlies experimentally well-established motor
94 adaption and history effects under changing contexts.

95 Results

96 Using the sCOIN model, we simulated representative experiments from a number of
97 experimental studies on motor adaptation to illustrate how this model explains different
98 experimental findings using the dynamics of context inference. We will present these sim-
99 ulations alongside the experimental results from the representative studies and discuss in
100 detail how context inference explains the experimental phenomena.

101 Before presenting these results, we briefly describe the COIN model and the simplifi-
102 cations that led to the sCOIN version used in simulations. We leave a more thorough
103 explanation of the models for the methods section. Additionally, we present simulations
104 using the sCOIN model that show the effects of contextual cues and perceptual noise on
105 context inference, which pave the way for the simulated experiments that we show later on.

106 Experimental designs

107 In the following sections, we discuss the experiments done by Kim et al. (2015), Oh and
108 Schweighofer (2019), Davidson and Wolpert (2004) and Vaswani and Shadmehr (2013). In
109 all experiments, participants are asked to do shooting movements from a starting position
110 to a known target, and the experimental manipulations can be clasified into two categories:
111 (1) curl forces with mechanical arms, and (2) visuomotor rotations. In this section, we

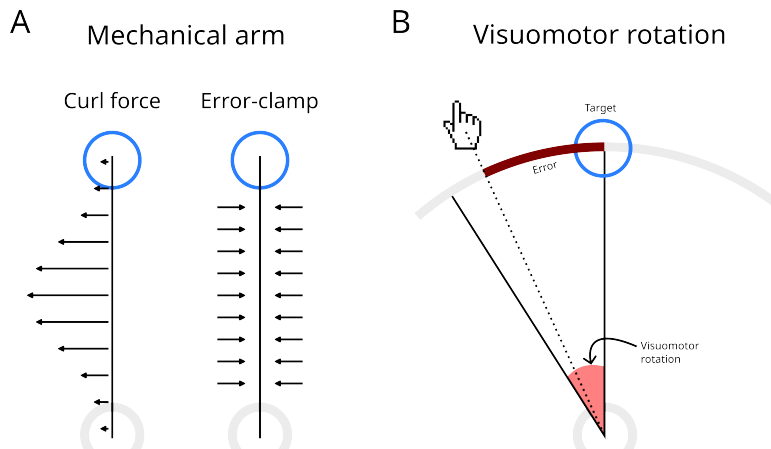


Figure 1. Mechanical arm and visuomotor rotation experiments. Green and blue circles represent the starting point and the target, respectively. Targets are place on the circumference on both experimental paradigms. (A) Mechanical arm experiment. During adaptation trials, the force exerted by the arm on the handle pushes the hand away from the straight line. In error-clamp trials, the mechanical arm creates resistance against movements perpendicular to the straight line to the target. (B) Visuomotor rotation experiment. Correspondence between hand movements and the cursor is rotated (visuomotor rotation). The error is measured as the arc between the target and the place at which the trajectory (dotted line) crossed the circumference.

112 briefly describe these two manipulations and leave the details of the experimental design to
113 the sections below where each study is discussed.

114 In experiments with mechanical arms, participants perform the movements while holding
115 the handle of a mechanical arm; the arm exerts a force on the handle on each trial which
116 depends on the speed of the participant’s hand, creating a force that is perpendicular to
117 the direction of movement, called a curl force (see Figure 1A). In these experiments, the
118 participants’ view of their hand and the mechanical arm is blocked, and they have to rely
119 on a representation of their hand on a screen in front of them, which includes the starting
120 position and the target. The experiments by Davidson and Wolpert (2004); Vaswani and
121 Shadmehr (2013) provide an accurate position of the participant’s hand, with no noise added
122 to it, and the cursor representing the hand is visible throughout the experiment; note that
123 Vaswani and Shadmehr (2013) added noise to the cursor on the screen during their third
124 experiment, but only their first experiment is simulated here.

125 When the mechanical arm is set to exert no force, movements made by human partic-
126 ipants are close to straight lines between the starting position and the target. When the
127 curl force is applied, movements deviate from this straight-line path, creating curved move-
128 ments that nevertheless reach the target, as participants adjust their trajectory before the
129 end of the movement. As participants repeat the movements over many trials, they learn to
130 adapt to these curl forces and go back to performing near straight-line movements. During
131 error-clamp trials, the mechanical arm engages a very stiff spring that causes participants’

132 movements to be a straight line, regardless of the participants' applied forces (see Figure
133 1A). This allows experimenters to present a zero-error feedback to the participant, while at
134 the same time measuring the forces they applied onto the spring.

135 Because participants can see the cursor, they can adapt their movement in flight, always
136 reaching the target. Errors are measured as deviations from the straight line connecting
137 starting and target positions.

138 In experiments with visuomotor experiments, participants move a cursor on a screen by
139 using a joystick Kim et al. (2015), or on the surface of a mirror using the pen of a digitizer
140 pad Oh and Schweighofer (2019). Movements are done from a starting position in the middle
141 of the screen to targets appearing on a circumference of 10cm in radius. The experimental
142 manipulation takes the form of a rotation between the hand movements and the cursor of
143 the screen (see Figure 1B), centered on the starting position. A clockwise rotation of 20
144 degrees means that a hand movement forward will translate to a movement towards the
145 right on the screen or mirror. Kim et al. (2015) uses the convention that clockwise rotations
146 are negative, while Oh and Schweighofer (2019) uses the opposite.

147 Oh and Schweighofer (2019) added Gaussian noise to the visuomotor rotation at each
148 trial. With this, each trial had a different visuomotor rotation, centered at 10 or 20 degrees,
149 and with a standard deviation of 0.5 or 4 degrees, depending on the condition. In this
150 work, we focused in the comparison between conditions 1a and 3, with means of 20 and 10
151 degrees, respectively, and standard deviation of 0.5 degrees.

152 In contrast to experiments with a mechanical arm, movements in visuomotor rotation
153 experiments are always close to a straight line. Errors are measured in degrees, as the
154 deviation between the target and the point in the 10cm circumference where the cursor
155 crossed it.

156 Modeling context-dependent adaptation

157 We focused on three main components of the COIN model: (1) context inference, (2)
158 motor adaptation and (3) action selection. The processes defined by these components
159 occur in this order, and each component informs the ones that follow.

160 Central to the model is the concept of context, defined in terms of the task to be per-
161 formed, the variables of the environment that are relevant to perform the task, the forward
162 models used by the decision-making agent to perform the task, and the update mechanisms
163 necessary to adapt these forward models to the changing environment. Together, these
164 elements allow the agent to make predictions on future observations when this context is
165 active, and these predictions are used to infer the context. For example, when lifting an
166 object of unknown weight, an agent might have learned one context for heavy objects and
167 one for light objects. When observing an object to be lifted, the agent can use its size and
168 texture to estimate the weight of the object, which in turn allows the agent to infer the
169 appropriate context and, with it, decide how to lift the object.

170 The COIN model contains, additionally to these three main components, components
171 for learning new contexts (i.e. inferring the existence of a new context that had not been
172 previously encountered by the agent), as well as the ability to infer subject-specific param-
173 eters such as a participant's assumed transition probabilities between contexts, which can
174 differ from the real, hidden transition probabilities. Because we sought to focus on switching
175 behavior between previously-learned contexts, as well as in the perceptual aspect of context
176 inference, we chose to fix the participant-inferred transition probabilities between contexts,
177 as well as the total number of contexts; in our simulations, we assume that participants have
178 already inferred the real values of these quantities. Because we mainly focus on switching
179 behavior, as well as error-clamp trials (both of which involve already-learned adaptations),
180 these simplifications to the model have minimal effects on our results. See Methods for
181 more details on the sCOIN model, as well as the differences between COIN and sCOIN.

182 By fixing the aforementioned values, the sCOIN model has a simpler generative model
183 which allows the agent to perform exact Bayesian inference for motor adaptation. The
184 inference process can be seen in Figure 2A, including the priors for both context inference
185 and motor adaptation. For more details on these choices, see the Methods section.

186 Contextual cues and feedback

187 The behavioral phenomena which are the focus of this work can be explained as arising
188 from the effects of contextual cues and sensory feedback provided to participants during
189 the experiment. To illustrate these effects in a simple example, we first simulated a generic
190 motor adaptation experiment similar to those performed by Davidson and Wolpert (2004):
191 participants performed reaching movements from a central position to fixed targets on a cir-
192 cumference, then back to the central position. All targets were positioned on the horizontal
193 plane, at shoulder height. Movements were performed holding a robotic arm which exerted
194 velocity-dependent rotary forces, which, when ignored, would move the participant's hand
195 away from the straight-line path to the target. See the following section for more details on
196 the experiments by Davidson and Wolpert (2004). The results of these simulations can be
197 seen in Figure 2B.

198 The key to an intuitive understanding of the results presented below is to observe what
199 happens when the presence and reliability of contextual cues is varied, as well as the percep-
200 tual noise on the position of the hand. To do this in our simulations, we added noise to the
201 categorical variable that encodes contextual cues, and to the observations (see Methods for
202 details), at two different levels (low and high noise). We simulated 50 participants, with 30
203 trials per participant. In Figure 2B, a 2x2 grid of results is shown: each simulation in this
204 grid is a combination of low or high contextual cue uncertainty (where high uncertainty is
205 equivalent to presenting no cues), and low or high perceptual noise (representing how well
206 participants can detect deviations from the straight-line movements).

207 Figure 2B shows that, in the presence of reliable contextual cues, context inference is
208 accurate, certain and fast to switch. However, as contextual cues become less reliable,
209 switching between known contexts becomes slower, as seen in the posterior probabilities

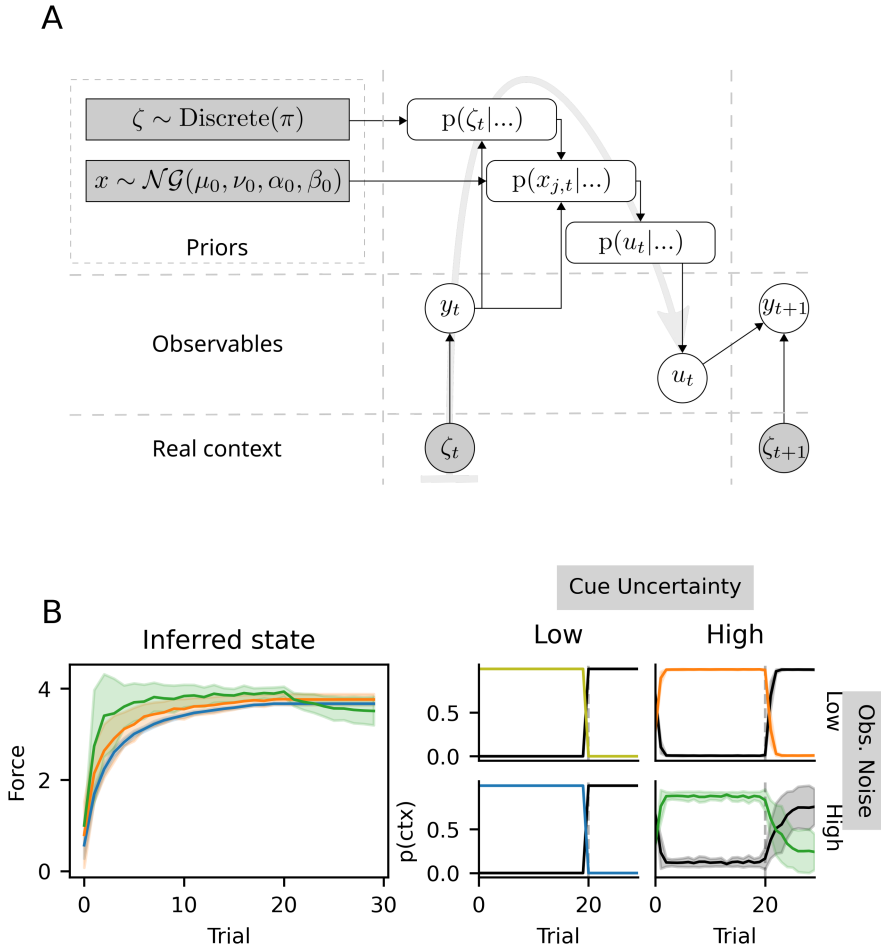


Figure 2. Schematic representation of the sCOIN model and illustrative simulations. (A) Inference done by the model at every trial. Clear circles represent the observables, i.e. the information available to the model (and the brain), and used for adaptation: motor commands u_t and direct observations y_t (e.g. cursor position). The true context ζ_t is not directly observable, but influences y_t . The dark rectangles represent the prior distributions for the inferred adaptation level x_t (Normal-Gamma distribution) and the current context ζ_t (discrete distribution with known π ; see Methods). At every trial, the context is inferred, then motor adaptation is carried out and finally a motor command is issued; the flow of this process is indicated by the gray arrow in the background, while black arrows show the direction of information flow. (B) Simulations obtained with the model in (A), using a simulated experimental setup similar to that by Davidson and Wolpert (2004), in which the context changes at trial 20 (vertical, dashed lines). A total of 2x2 experiments were simulated, with low and high levels of both cue uncertainty and observation noise. In the left panel, the states inferred by the model for each of the 2x2 simulated experiments, where each color represents one experiment, with the same colors as the panels on the right. On the right, each plot represents context inference $p(\zeta_t)$ for one specific level of cue uncertainty and observation noise. The y-axis represents the posterior probability of each context $p(\zeta_t = j)$; the black line represents the baseline context (i.e. no adaptation), the colored line (with the same colors as the panel on the left) represents the only adaptation to be learned during the simulated experiment. The shaded areas represent the standard deviation around the mean, obtained across 50 simulated participants.

210 over contexts at and after trial 20 in the last column. Furthermore, as perceptual noise
 211 increases, switching becomes not only slower, but also more uncertain, with individual
 212 agents incorrectly missing the switch entirely. While cue uncertainty and observation noise
 213 have an effect on the motor adaptation process, as seen on the left-most panel in Figure
 214 2B, in all simulations the hidden state (i.e. the force exerted by the mechanical arm, $x_{j,t}$)
 215 is quickly inferred.

216 As we show below, these effects are at the heart of the behavioral phenomena observed in
 217 the experiments by Kim et al. (2015), Oh and Schweighofer (2019), Davidson and Wolpert
 218 (2004), and Vaswani and Shadmehr (2013), and our simulated data qualitatively matches
 219 their results, as well as others that we discuss in the Discussion section.

220 Experimental results

221 In this section, we present experimentally-observed phenomena in three sections, and
 222 show that the dynamics of context inference provide a unifying explanation for all of them.
 223 In the first section, we discuss switches between contexts, and how slow context inference
 224 affects these switches. In the second section, we focus on interference between learned
 225 adaptations. Finally, in the third section we discuss context inference during error-clamp
 226 trials, and its effect on behavior. For each of the three sections, we selected one or two
 227 studies which are representative of the phenomenon being discussed.

228 For clarity, we first introduce necessary terminology that is typically used in experimen-
 229 tal studies. As an example, we will use a typical motor adaptation task in which participants
 230 have to make reaching movements while holding the handle of a mechanical arm that exerts
 231 a curl force on the participant’s hand. Depending on the trial, the mechanical arm might
 232 exert a curl force in a clockwise or counter-clockwise direction, or no force at all. Let us
 233 define the baseline context O as that in which the mechanical arm exerts no force. Contexts
 234 A and B can be defined as those with clockwise and counter-clockwise forces, respectively.
 235 Abusing notation, a usual statement is that $B = (-A)$, as the forces have the same magni-
 236 tude but point in opposite directions. Similarly, one can define context $A/2$, with the same
 237 direction of adaptation as A , but half the magnitude. Finally, many experiments include a
 238 block of error-clamp trials at the end of the experiment, in which the mechanical arm forces
 239 the participant’s hand into a straight-line trajectory towards the target by counteracting
 240 any lateral forces, eliminating any error for the trial; we represent these with the letter E .

241 With this terminology, a typical experiment (e.g. Ethier et al., 2008) would have a block
 242 structure of $O - A - B - E$, or $O - A - (-A) - E$, which means that the participant
 243 goes through a block of trials with no external force applied (O), a number of trials with a
 244 clockwise curl force (A), a block with counter-clockwise forces (B), and finally a block with
 245 error-clamp trials (E). When participants are exposed to the same context multiple times
 246 (e.g. Oh & Schweighofer, 2019), an experiment can be described as $O_1 - A_1 - O_2 - \dots$,
 247 where A_n is context A , presented to the participant for the n -th time.

248 **Cue- and sensory feedback uncertainty affects switching behavior.** The term
249 'savings' refers to the ability to remember a previously-learned adaptation, observed as an
250 instant recall of the previously-learned adaptation (e.g. Kim et al., 2015; Oh & Schweighofer,
251 2019), or as accelerated re-learning (e.g. Kojima, Iwamoto, & Yoshida, 2004); in the case
252 of instant recall, the phenomenon is often called 'switching'. Savings is almost universally
253 observed in humans (Brashers-Krug, Shadmehr, & Bizzi, 1996; Medina, Garcia, & Mauk,
254 2001; Shadmehr & Brashers-Krug, 1997; Smith et al., 2006; Zarahn, Weston, Liang, Maz-
255 zoni, & Krakauer, 2008). In an $O - A - O - A$ experiment, for example, savings would
256 express themselves in the second A block in the form of a much higher adaptation rate than
257 that observed during the first A block. The related concept of quick de-adaptation occurs
258 in $A - O$ transitions, where participants switch back to baseline without having to re-learn
259 it.

260 In this section, we discuss savings in terms of switching between contexts. We show that
261 through context inference and how it is affected by contextual cues and observation noise,
262 savings are not immediate, but a relatively fast process that reflects context inference. In
263 particular, we show that the manifestations of savings on behavior are mediated by context
264 inference, which could mask the presence of savings in cases where observations do not
265 unequivocally identify a context.

266 To show this, we examined multiple experimental studies in which savings are observed.
267 We categorized these studies based on the amount of contextual information made available
268 to participants: In some experiments (e.g. Kim et al., 2015; Lee & Schweighofer, 2009), the
269 context is clearly revealed to the participant using sensory cues. We call these cued-context
270 experiments. In other experiments, partial information is available to participants (e.g.
271 Davidson & Wolpert, 2004; Zarahn et al., 2008) in the form of large prediction errors,
272 partial contextual information or reward prediction errors; we refer to these as partially-
273 cued experiments.

274 We selected three representative experiments from two studies (Kim et al., 2015; Oh &
275 Schweighofer, 2019) which differ in the amount of contextual information available to par-
276 ticipants. Kim et al. (2015) performed a cued-context visuomotor rotation experiment with
277 three contexts with different rotation: no rotation, 40 degrees and -40 degrees. Participants
278 performed shooting movements in blocks of trials with the same rotation. Importantly, a
279 colored light identified the current context, making this a cued-context experiment. Con-
280 sistent with the context-inference account, the authors found that switching was immediate
281 and accurate.

282 In Figure 3A we show the results of simulations with the model using the parameters
283 of the task, as well as the experimental results from Kim et al. (2015). The correspondence
284 between simulations and experimental results can be seen in the switches between contexts
285 in the third and fourth columns, where the solid gray line (representing the true context)
286 switches between 40, 0 and -40, and the thick black line, representing the agent's adaptation,
287 quickly follows these switches.

288 In the second panel of Figure 3A, we show the inferred state (i.e. the inferred angle

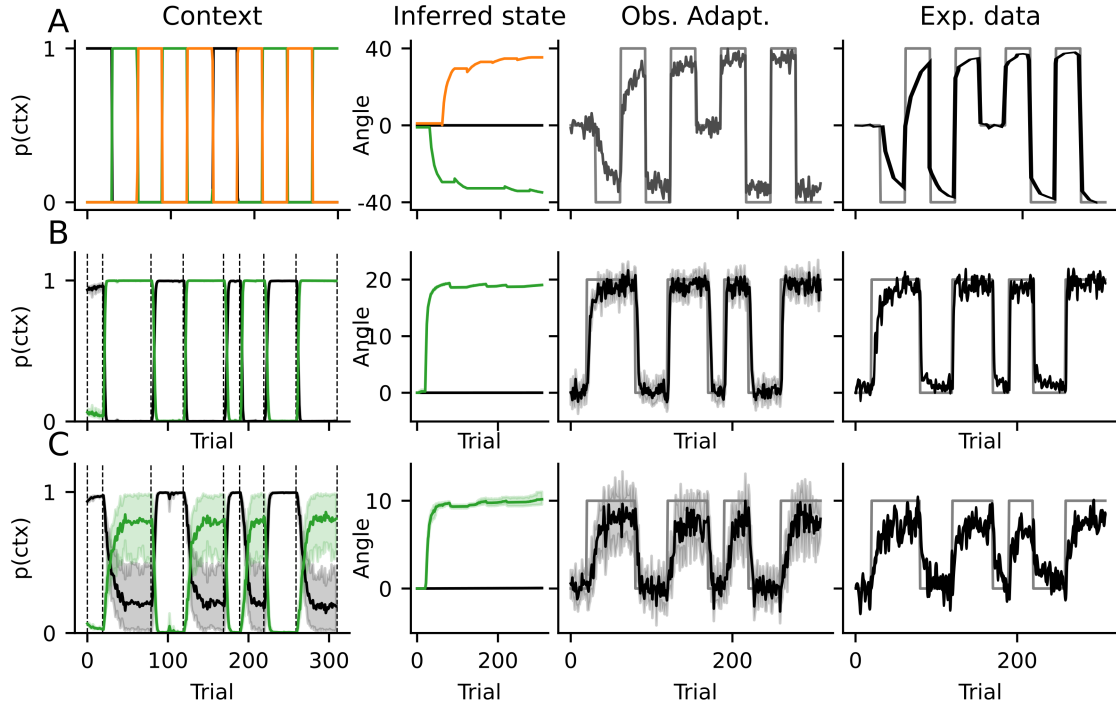


Figure 3. Switching between learned adaptations gated by context inference. Data from our simulations (first three columns) compared to data adapted from figure 2A by Kim et al. (2015) and figure 4A from Oh and Schweighofer (2019) (last column). Experimental and simulated data was, in all three experiments, averaged across all participants. In the first column, the simulated context inference is represented by the posterior probabilities over all available contexts. Each color (black, orange, green) represents a different context, with black always representing the baseline (i.e. no adaptation). Vertical, dashed lines represent switches in the real context. The inferred state (angle of the visuomotor rotation) is shown in the second column, with the same colors as in the first column. In the third and fourth columns, the black line represents the adaptation (i.e. response) displayed by the agent as a function of trial number. The thin gray lines represent the optimal adaptation, i.e. the size of the true visuomotor rotation during the task. (A) Experiment by Kim et al. (2015). Both experimental and simulated results are shown only up to trial 300, of the original 600. (B) An experiment by Oh and Schweighofer (2019). Blue and black lines are as in A. (C) Same experiment as (B) but with a 10 degree adaptation.

of rotation). Critically, it can be seen for the first four context switches (until about trial 200) that participants had not yet completely adapted to the rotation, as also evidenced by their responses not being on par with the true rotation angle. This undershooting of responses (i.e. not doing the 40 degree rotation) happens despite participants being able to immediately and with high certainty identify the true context, as shown in the first-column panel. These results are similar to those shown by Imamizu et al. (2007), where sensory cues of varying reliability effected immediate or slow contextual switches.

To expand on these results, we now turn to feedback and its effects on switching behavior. Oh and Schweighofer (2019) performed two partially-cued experiments with a visuomotor rotation of 20 and 10 degrees, respectively. The results of their experiments can be seen in Figure 3B and 3C, alongside simulations with the sCOIN model. Participants in the first experiment (Figure 3B) first learned the adaptation in *A*. In subsequent context transitions, participants showed immediate switching (with a one-trial lag) between *A* and *O* (both ways), which can be seen in their responses (black line in the last two columns of Figure 3B) closely following the switches in the true rotation. In the second experiment (Figure 3C), context switching happens more slowly, with adaptation lagging behind the switches in the real context, and slowly catching up. As can be seen in the left panels in Figure 3B and 3C, the same model parametrization produces fast, accurate switches when the adaptation is large (B), and slow, noisy switches when it is low (C). This difference is explained in our simulations in terms of the size of the adaptation in relation to observation noise: as the adaptation is smaller (10 degrees), it becomes more difficult to distinguish errors made by incorrectly inferring the context from the noise due to trial-to-trial variation in motor output. Because of this, the model requires more evidence (i.e. more trials) to infer a switch in contexts.

In contrast, Oh and Schweighofer (2019) explained the results of their second experiment by positing that when adaptations were small, participants did not identify this as a new context and opted instead for a modification of their baseline model (i.e. how they move normally). Under this single-context explanation, however, savings do not exist, and adaptations need to be learned anew every time a context changes. On the other hand, savings are present under the sCOIN model, their manifestations being diminished by the slower context inference. Oh and Schweighofer (2019) analyzed savings during their second experiment and found that savings do exist, although greatly diminished compared to the first experiment. This is in favor of the dual-context model, as we present it here. Oh and Schweighofer (2019) showed a slow decay during error-clamp trials in their experiments, which they considered evidence for the single-context account of the second experiment. However, as we show below, this can also be explained in a dual-context model as an effect of slow context inference.

Uncertainty over contexts affects action selection. As with learning, we show in this section that action selection is affected by context inference. If the identity of the current context is known, the forward model for this context is used to select the current action. However, if uncertainty over the context exists, the selected action is influenced by all the possible contexts, with a weight directly related to how likely each one of those contexts is (see Equation 6).

332 Experimental evidence supporting this view can be found in experiments with context
 333 switching. For example, Davidson and Wolpert (2004) reported a curl-force experiment in
 334 which participants had to switch between A and $3A$ in one group, with a block sequence
 335 $A - 3A - A - 3A$, and from A to $-A$ in another group, with a block sequence $A - (-A) -$
 336 $A - (-A)$. After A and $3A$ (or $-A$ in the other group) had been learned in the first two
 337 blocks, the authors found that the switch from $3A$ to A was faster than that from $-A$ to A .
 338 The authors interpreted this as evidence that switching between adaptations happens more
 339 quickly if it is in the same direction as the current adaptation (e.g. both counter-clockwise),
 340 and more slowly if they are in the opposite direction (e.g. clockwise to counter-clockwise).

341 Under the sCOIN model, the asymmetry is caused by the existence of the baseline
 342 context, which has a non-zero probability $p(\zeta_O|s_t\dots)$, as can be seen in Figure 4A. When a
 343 new block of trials starts (e.g. in the transition from $3A$ to A), a switch is inferred by the
 344 model (given feedback after the first trial) and ζ_O becomes more likely (given that ζ_{3A} has
 345 been ruled out). Therefore, in these first trials, action selection has a component guided by
 346 the baseline model, in which no extra compensatory force is applied, effectively “pulling”
 347 adaptation towards zero (no compensatory force). In the first group, this initial pull towards
 348 zero accelerates the transition towards A because $3A > A > 0$, but in the second group,
 349 it slows down the switch because $A > 0 > -A$ and the behavior lingers around 0 until
 350 $p(\zeta_0|\dots)$ drops back to zero.

351 To confirm this explanation, we simulated variants of the experiment in which the sCOIN
 352 model predicts that the difference between groups diminishes or disappears. First, in Fig-
 353 ure 4B, we simulated an experiment in which the contexts have more extreme adaptations,
 354 making them more different from baseline than in the Davidson and Wolpert (2004) ex-
 355 periments. To do this, one group adapts in a $O - A - (-2A)$ paradigm, while the other
 356 group adapts in a $O - A - 4A$ paradigm. As in the original experiment, the second contexts
 357 ($-2A$ for one group, $4A$ for the other) are equally spaced from the first context. However,
 358 given the larger distance from baseline, the baseline context has the same probability for
 359 both groups after the switch back to A . This change makes both simulated groups infer
 360 the correct context almost equally quickly, making the difference between their errors much
 361 smaller compared to the original experiment. Furthermore, we simulated an experiment
 362 with an identical structure to that of Davidson and Wolpert (2004), but eliminated the
 363 baseline context from the agent. The results can be seen in Figure 4C, where the switches
 364 between contexts are made identically by the two groups.

365 **Action selection in error-clamp blocks.** During error-clamp blocks at the end
 366 of block sequences, participants’ behavior can be divided in two phases: (1) Participants’
 367 behavior is consistent with a previously-encountered context (called spontaneous recover
 368 in $O - A - B - E$ experiments, where behavior is consistent with A); this phase, when
 369 present, is seen during the early trials of the E block. (2) A slow return to baseline, which
 370 can last as long as hundreds of trials (Brennan & Smith, 2015). However, the direction of
 371 adaptation during the first phase, its duration, the delay before it is observed, the speed of
 372 the return to baseline and the final asymptote of the response vary greatly depending on
 373 the experiment (Brennan & Smith, 2015; Shmuelof et al., 2012; Smith et al., 2006; Vaswani
 374 & Shadmehr, 2013).

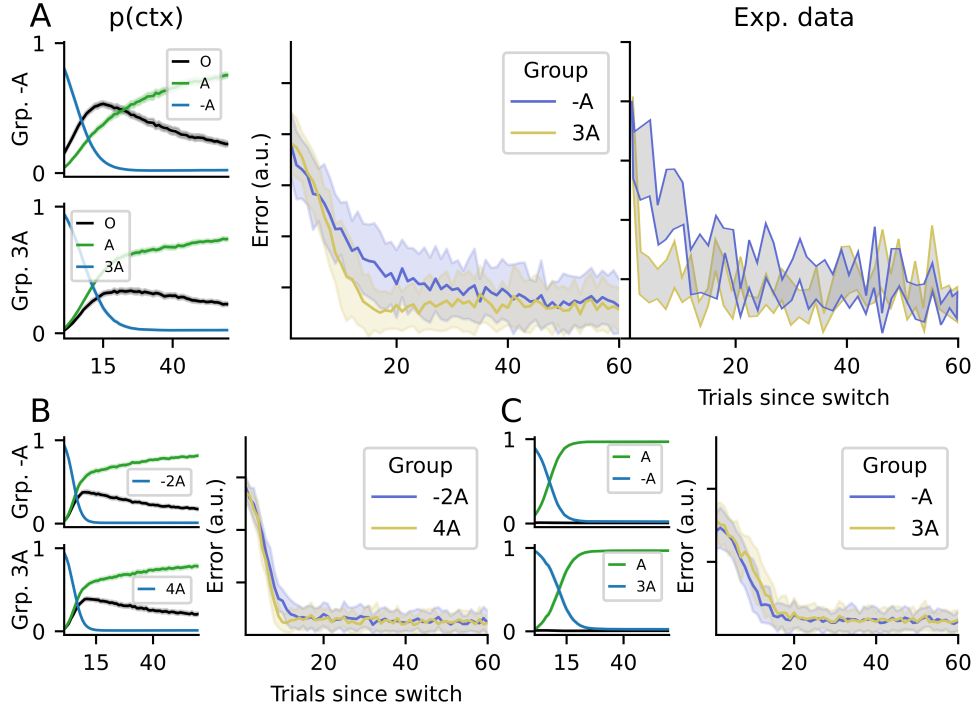


Figure 4. Motor error when switching back to a previously-learned adaptation. (A) Experimental results from Davidson and Wolpert (2004) and simulations with the sCOIN model are shown. In the first column, each panel represents context inference for one group of participants (top: group $-A$; bottom: group $3A$), with each line representing the posterior probability of a context (black for the baseline O). The second column represents the error made by our simulated agent after returning to the previously-learned context, with blue and yellow representing groups $-A$ and $3A$, respectively. The last panel represents the same data, from the Davidson and Wolpert (2004) experiment. All panels share the x-axis, representing the number of trials elapsed since the switch to the new context. All simulations were executed 32 times per group, to obtain a reliable mean; shaded areas represent the standard deviation across all simulations. (B) Simulated results for an experiment similar to Davidson and Wolpert (2004), but changing the contexts seen by the two groups from $-A$ to $-2A$ for the first group, and from $3A$ to $4A$ for the second group. The panels follow the same structure as (A), without the last panel for experimental results. (C) Simulations for an experiment in which the baseline context has been removed altogether.

375 In this section, we show how context inference can explain these different parameters
 376 of behavior by changing the way contextual cues mislead participants' context inference,
 377 which in turn influences action selection.

378 This can be seen for example in (Vaswani & Shadmehr, 2013), where the authors studied
 379 in detail human behavior during an error-clamp block in a shooting movement paradigm
 380 with a mechanical arm. The authors found that during an *E* block at the end of each
 381 experiment, there was a lag of a few trials (depending on participant) before their motor
 382 behavior changed from that of the previous block. After that, the exerted force slowly
 383 dropped towards zero throughout tens of trials, but never reaching values around zero.
 384 Participants were divided into four groups, each of which going through a different block
 385 sequence: (1.1) $A - E$, (1.2) $O - A - E$, (1.3) $(-A/2) - A - E$, and (1.4) $(-A) - E$. No
 386 pauses were made during the experiment nor were there any contextual cues, so transitions
 387 between blocks were not signaled to participants. However, because context inference inte-
 388 grates information from different sources, many experiments in which no intentional, overt
 389 contextual cues are available indeed contain contextual information that the participant
 390 can use to infer the context. For example, proprioceptive signals provide contextual infor-
 391 mation (Dizio & Lackner, 1995; Shadmehr & Mussa-Ivaldi, 1994). The sudden appearance
 392 of motor errors can itself be a cue for contextual change (Herzfeld et al., 2014) and even a
 393 pause between two trials could suggest a change in context (Ethier et al., 2008).

394 In Figure 5A, we show data simulated with the sCOIN model, following the parame-
 395 ters of the experiment by Vaswani and Shadmehr (2013), and in Figure 5B we show the
 396 experimental plots adapted from Vaswani and Shadmehr (2013). As in the experiments
 397 by Vaswani and Shadmehr (2013), we simulated error-clamp trials by forcing the observed
 398 error to zero, regardless of the action taken by the model. The displayed adaptation is
 399 shown during the *E* trials for the three experimental groups in the experiment. It can be
 400 seen that group 1.3 (i.e. the participants who had learned in the $-A/2$ context in addition
 401 to A) more quickly recognized a change in context and lowered the force applied on the
 402 mechanical handle, as can be seen in the experimental data.

403 In Figure 5C, the inference over context is shown for each group separately. Context
 404 inference works reliably until the error-clamp trials start, which do not correspond to any
 405 of the known contexts. This causes the agent to infer the combination of some of the known
 406 contexts that best fits the observations. Depending on the contexts previously learned by
 407 the agent: groups 1.1 and 1.4 display the same behavior, where the previous context (A
 408 and $-A$, respectively) slowly dwindle. These agents will slowly lower the force applied. In
 409 contrast, group 1.3 has learned the additional $-A/2$ context, which has a non-zero posterior
 410 probability during *E* trials, pushing the agent's adaptation force more quickly towards zero.
 411 Group 1.2 behaves similarly to 1.1, with the exception that the baseline context, which was
 412 recently seen, plays a bigger role during *E* trials, making the agent reduce its force during
 413 *E* trials slightly more quickly than groups 1.1 and 1.4.

414 Vaswani and Shadmehr (2013) also found participant-specific delays before the decay
 415 to baseline started after the error-clamp phase began. As can be seen in Figure 5D, each
 416 simulated participant follows a different path of decay, with variations caused directly by

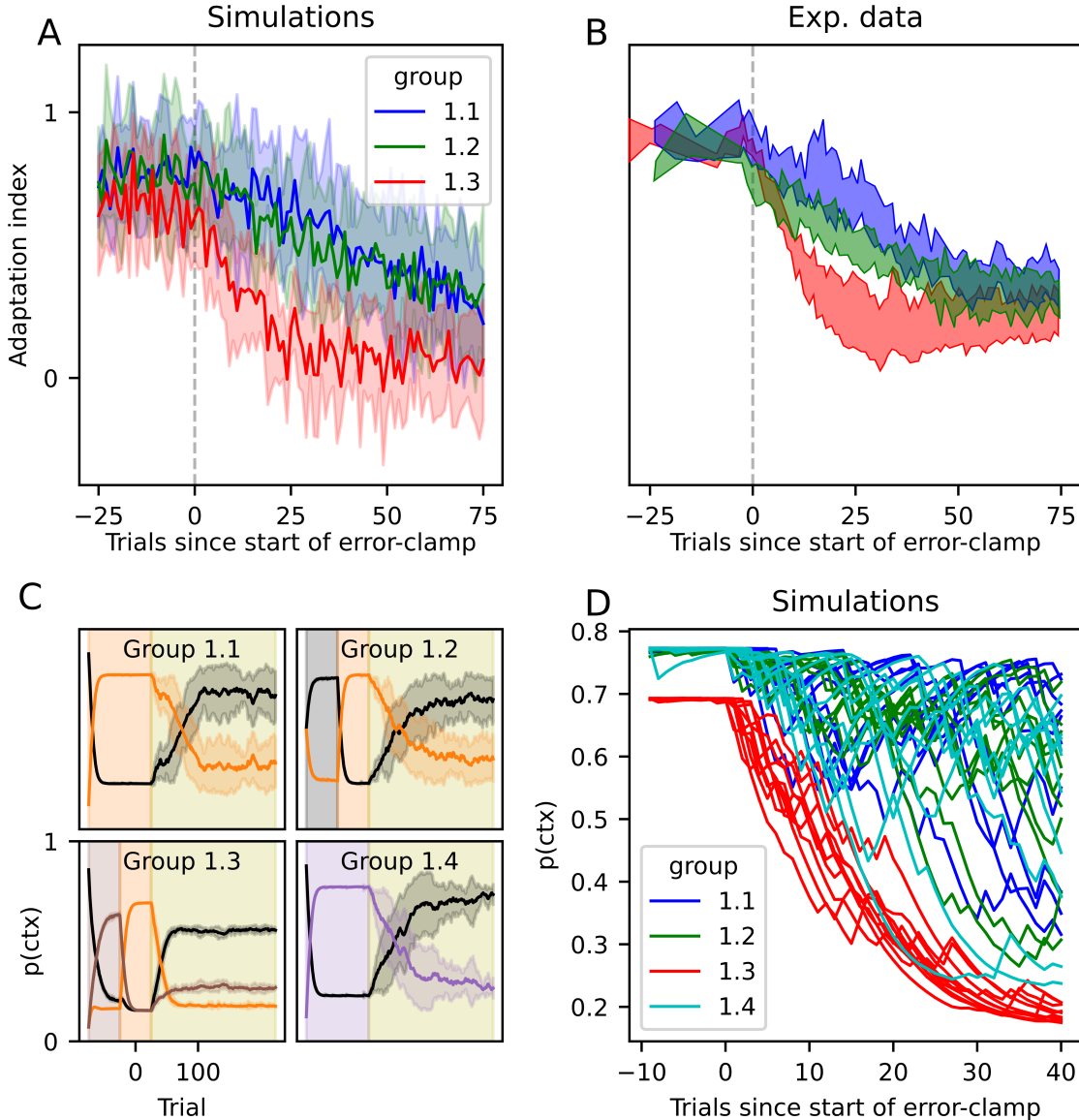


Figure 5. Adaptation during error clamp trials. (A) Simulated adaptation during the error-clamp trials for the three groups of participants in Vaswani and Shadmehr (2013), using the same colors. Following Vaswani and Shadmehr (2013), group 1.4 is not shown in A and B, as their behavior is identical to group 1.1. The solid line is the average across 10 runs (i.e. a group of 10 simulated participants) and the shaded area represents the standard deviation. The vertical dashed line is the start of the error-clamp trials. (B) Corresponding experimental data adapted from figure 2C by Vaswani and Shadmehr (2013). (C) Simulations: Inference over the current context, where contexts are color coded: black for baseline, orange for the counter-clockwise force, purple for the clockwise force and brown for counter-clockwise force with half strength. The lines represent the posterior probability of each context in every trial, while the background color represents the true context. An olive-colored background represents error-clamp trials. As in (A), solid lines represent the average across all runs and shaded areas represent the standard deviation. (D) Simulations: Visualization of the lag before a change in context is detected by the agent during the E trials. Each line represents one run (10 runs per group).

417 perceptual noise. In our simulations, however, it is clear that no such systematic lag can
418 be directly observed, which is most noticeable when looking at context inference (Figure
419 5C), which begins the switch as soon as the error-clamp trials begin. This can be further
420 observed in Figure 5D, where we plot each simulated participant (one run of the simulations,
421 color coded as before); because observation noise was chosen randomly for each run, some
422 runs appear to contain a large delay before the decay begins. This falls in line with the
423 experiments by Brennan and Smith (2015), who found that the lag observed by Vaswani
424 and Shadmehr (2013) disappeared when controlling for correlations in perceptual noise, as
425 well as by using a balanced experimental design and unbiased analysis.

426

Discussion

427 We showed that context inference as an active, continuous process, can explain many
428 behavioral phenomena observed experimentally. In particular, we showed that the effects
429 of the presence and reliability of contextual cues, as well as observation noise, can cause
430 behavior that can be observed during context switching, as well as during times in which
431 context inference is hindered, as is the case during error-clamp trials in many experiments.

432 To do this, we selected representative experimental studies that show the well-established
433 effects of savings, spontaneous recovery and the effects of sensory cues. Using a simplified
434 version of the COIN model introduced by Heald et al. (2021), we showed how each of
435 these effects can be explained by the dynamics of context inference, which integrates all the
436 available information (e.g. sensory cues, workspace location, reward and endpoint feedback),
437 in some cases throughout many trials.

438 With this, we expanded on previous works that introduced the idea that context in-
439 ference is a process that informs and is informed by motor adaptation by showing that
440 it explains behavioral phenomena that had previously required different specific, ad-hoc
441 mechanisms outside of contextual motor adaptation.

442 **Further experimental evidence**

443 In many cases, the context is not directly observable and context inference takes the
444 form of an evidence-accumulating process that can take any amount of time to be sure of
445 the context. It is in these cases where the effects of context inference are most noticeable.
446 While many experiments exist that give probabilistic contextual information (e.g. Behrens,
447 Woolrich, Walton, & Rushworth, 2007; Nassar, McGuire, Ritz, & Kable, 2019; Scholz &
448 Schöner, 1999), evidence accumulation is not limited to these explicitly stochastic cases.
449 Indeed, as we noted in the Results section, many experiments inadvertently include partial
450 contextual information used by participants.

451 The most direct secondary contextual information comes in the form of reward and end-
452 point feedback. For example, participants may be told whether they obtained the desired

453 reward at the end of a trial and are shown the end point of their movement. When participants
454 observe an unexpectedly large error, they can infer that the inferred context might
455 be incorrect. This is the case of the experiments by Oh and Schweighofer (2019) shown
456 in Figure 3B-C: if the adaptation is high, changes in context produce errors much larger
457 than those of motor variability, and a context switch is easily and immediately identified;
458 if adaptation is low, the errors produced by context switching are closer in magnitude to
459 motor variability and evidence accumulation is necessary.

460 The same rationale explains the results by Herzfeld et al. (2014), as was shown by Heald
461 et al. (2021): motor learning, which in the COIN model is modulated by context inference,
462 is minimal for errors close to 2 and -2 (see their figure 2E). This is because an error of
463 2 or -2 signals that the participant incorrectly identified the context (as adaptation has
464 a magnitude of 1). Additionally, as was shown by Heald et al. (2021), context inference
465 explains the modulation of learning rate by the volatility of the environment observed by
466 Herzfeld et al. (2014).

467 A subtler source of information can be found in long pauses between blocks of adaptation
468 trials, after which an unprompted partial return to baseline has been observed (Ethier et al.,
469 2008). This can be explained by context inference, as a long pause could prompt participants
470 to infer that a switch had occurred, prompting participants to rely on their belief of the
471 underlying probability of observing any of the known contexts, which is dominated by the
472 previously observed context A , but now includes a component of the baseline O , as it is the
473 most common one in everyday life.

474 Error-clamp (E) trials present another insight. If error is kept at zero, one could assume
475 that participants would continue doing what they were doing before, as there is no reason
476 (no observed error) to infer a change in context. However, this is almost never the case (e.g.
477 Ethier et al., 2008; Forano & Franklin, 2020; Pekny, Criscimagna-Hemminger, & Shadmehr,
478 2011; Scheidt, Reinkensmeyer, Conditt, Rymer, & Mussa-Ivaldi, 2000; Smith et al., 2006;
479 Vaswani & Shadmehr, 2013). Instead, participants slowly reduce their adaptation, often
480 displaying spontaneous recovery (e.g. Smith et al., 2006). Context inference provides a prin-
481 cipled account of this behavior: the natural variability in participants' behavior lead them
482 to expect errors, which clashes with the observed zero error. This prompts participants to
483 re-evaluate their inferred context, which can partially activate a previously-observed con-
484 text, as we showed in Figure 5. Pekny et al. (2011) found similar results, demonstrating
485 that the duration of the previously-observed adaptation block also affects behavior in the E
486 block. Additionally, Criscimagna-Hemminger and Shadmehr (2008) showed that introduc-
487 ing long periods before the E block begins lowers the initial force that participants exerted
488 on the mechanical arm during the E block; longer periods of time make context inference
489 revert to the prior expectation that a new baseline block begins, because participants are
490 free to move their arm about during the pause.

491 In our account, if all information indicating a change in context is removed from the
492 experiment, participants would continue to behave as they were in the previous block.
493 Evidence for this can be seen in experiments 2 and 3 by Vaswani and Shadmehr (2013),
494 where participants were shown random errors during E trials, with a variance matching

495 that of previously observed motor commands. The authors showed that by matching the
496 errors expected by participants, they eliminated the slow tapering-off observed in most *E*
497 blocks.

498 **Model predictions**

499 The basic principle behind the results we presented is that the sCOIN model describes
500 a process that develops over time and that carries with it uncertainty. This uncertainty
501 affects learning and behavior during motor adaptation, effecting phenomena that are directly
502 observable during behavioral experiments. In the following, we discuss several testable
503 predictions that are direct consequences of the model.

504 For the model predictions discussed below, it is important to keep in mind that different
505 contextual cues are not equally effective at separating motor responses during learning and
506 switching (Howard, Ingram, Franklin, & Wolpert, 2012; Howard, Ingram, & Wolpert, 2010;
507 Imamizu et al., 2007). Because of this, the model predictions hinge on selecting the adequate
508 type of contextual information that maximally helps the participants select the appropriate
509 motor response.

510 **Error-clamp as a known context.** The inclusion of reliable sensory contextual cues
511 (e.g. lights whose color uniquely identify a context) makes switching immediate, as in the
512 experiments by Kim et al. (2015). We expect that the same effect would be observed in
513 error-clamp trials. If the *E* block is learned by participants during training, it might still
514 be difficult for them to infer that an *E* block has started, which would create delays similar
515 to those in Figure 5. However, the model predicts that if a visual cue is introduced that
516 identifies the *E* block, participants would immediately switch to their baseline behavior, no
517 longer displaying an adapted response, lag, nor the slow return to baseline. This imme-
518 diate switch in the presence of contextual cues would persist even if endpoint feedback is
519 manipulated as Vaswani and Shadmehr (2013) did.

520 Note that the original COIN specification includes a component to learn new contexts.
521 However, this component works exclusively by creating new contexts in which the forward
522 models take the same form but have different parameter values. New mechanisms would
523 be needed to allow the COIN model to create contexts in an online fashion that operate in
524 an essentially different manner, as is the case of error-clamp trials, in which participants'
525 responses do not affect the outcome and motor commands are issued based on criteria not
526 directly related to the goal of the task (e.g. energy minimization or comfort maximization).

527 **Interference effects during context switching.** As discussed in the Results section,
528 the effect observed by Davidson and Wolpert (2004) is explained by the model as an effect
529 of slow context inference, instead of being a direct interference at the level of learning.
530 As shown in Figure 4B-C, the context inference account predicts that this effect would
531 disappear if all contexts were significantly different from baseline, such that the baseline
532 context never explains the observations. Removing the baseline context from a participant's
533 context inference might be experimentally unfeasible, but other possibilities include making

534 all adaptations bigger (e.g. bigger angles, stronger forces), and including contextual cues
 535 that rule out the baseline context. In the opposite direction, the model predicts that if
 536 all adaptations are smaller (i.e. closer to baseline), the differences between the two groups
 537 would increase, although such differences might become impossible to detect due to different
 538 sources of noise in the data.

539 **Multi-source integration.** The model also predicts an effect reminiscent of multi-
 540 sensory integration (Ernst & Banks, 2002): in order to integrate contextual information
 541 from conflicting sources (e.g. probabilistic visual cues and noisy endpoint feedback), the
 542 weight placed on a source increases with its reliability. Such integration would manifest
 543 itself in experiments in which observations are noisy, as in the experiments by Kording and
 544 Wolpert (2004), in which the position of the finger was obscured and instead participants
 545 are shown a blurry cursor which was sometimes shifted from its real position. If the added
 546 observation noise gives evidence for a particular context (the true underlying context or an-
 547 other one) and a visual cue gave partial information for another context, the participants’
 548 behavior would be more consistent with the most reliable source of contextual information.

549 Conclusions

550 The results we presented in this work indicate that several well-established behavioral
 551 phenomena observed across different motor adaptation experiments can be explained by the
 552 uncertainty in context inference and its effects on learning and action selection. Together
 553 with the results by Heald et al. (2021), these results suggest new venues of investigation for
 554 future works in motor adaptation and context-dependent behavior.

555 Methods

556 The COIN and sCOIN models

557 In this work, we used a simplified version of the recently-introduced COIN model (Heald
 558 et al., 2021), adapted to the experiments that we covered in our simulations. In this section,
 559 we give a brief introduction to the COIN model and, in the subsequent subsection, describe
 560 how we adapted the model to the experimental tasks. For a full description of the model,
 561 refer to Heald et al. (2021).

562 **Generative model.** At each trial t , the agent infers both the context and the context-
 563 dependent adaptation (e.g. the parameters of the force field in mechanical-arm experi-
 564 ments). The context is represented by a latent, categorical variable ζ_t , which is assumed to
 565 evolve over time according to:

$$p(\zeta_t | \zeta_{t-1}, \pi_{\zeta_{t-1}}) = \text{Discrete}(\pi_{\zeta_{t-1}}) \quad (1)$$

566 where $\pi_{\zeta_{t-1}}$ is the transition probability vector from context ζ_{t-1} to all other contexts. The
 567 contextual cues (when present in an experiment) are assumed to be drawn depending on

568 the context following:

$$p(q_t|c_t, \Phi) = \text{Discrete}(\Phi_{\zeta_t}) \quad (2)$$

569 where Φ_{ζ_t} is the probability vector with which the contextual cue q_t is shown to the agent
570 in context ζ_t . As pointed out by Heald et al. (2021), both Φ and π are in principle infinite,
571 but a task-relevant finite set can be used instead.

572 The context-dependent adaptation is represented by the latent variable $x_{\zeta,t}$ and assumed
573 to arise from an autoregressive process AR(1):

$$x_{\zeta,t} = a_{\zeta}x_{t-1} + b_{\zeta} + \omega_{\zeta} \quad (3)$$

574 where a_{ζ} and b_{ζ} are unknown, context-dependent parameters and ω is a Gaussian noise
575 term of zero mean and unknown standard deviation $\sigma_{\zeta,x}$. This AR(1) process is assumed to
576 have existed before the experiment begins and to have a stationary Gaussian distribution
577 of unknown mean and variance:

$$p(x_{\zeta,t}) = \mathcal{N}(\mu_{\zeta,x}, \sigma_{\zeta,x}) \quad (4)$$

578 Note that $\mu_{\zeta,x}$ and $\sigma_{\zeta,x}$ are parametrized by the parameters of the AR(1) process, namely
579 $\mu_{\zeta,x} = d_{\zeta}/(1 - a_{\zeta})$ and $\sigma_{\zeta,x} = \sigma_q/(1 - a_{\zeta}^2)$, where σ_q is a free parameter of the model which
580 is not context dependent.

581 Observations take the form of state feedback (e.g. the position of the cursor on the
582 screen in visuomotor rotation tasks), given by:

$$y_t = x_{\zeta,t} + \nu_t \quad (5)$$

583 where ν_t is a zero-mean Gaussian noise term with unknown standard deviation σ_r , which
584 is a free parameter of the model.

585 Action selection (i.e. motor output u_t) is done via the weighted mean of $x_{j,t}$:

$$u_t = \sum_j p(\zeta_{j,t}|q_t...)x_{j,t} \quad (6)$$

586 where $p(\zeta_{j,t}|q_t...)$ is the predictive probability.

587 To include motor noise (independent from estimation uncertainty), as well as carry over
588 the uncertainty over $x_{j,t}$, we instead sample motor commands from a Gaussian centered on
589 this mean, with a standard deviation σ_u , which is a free parameter of the model.

590 **Simplified COIN model.** The free parameters of this model can be fitted to par-
591 ticipants' data, as was done by Heald et al. (2021). In this work, we instead chose values
592 for these parameters to show that the model is capable of explaining the experimental phe-
593 nomena in the Results section. Additionally, by fixing these parameters the agent is able to
594 perform exact Bayesian inference at each trial using conjugate priors, replacing the MCMC
595 approach used by Heald et al. (2021) due to the mathematical intractability of the full
596 formulation. This, however, does not significantly change the model and was done purely

597 for computational efficiency. In this section, we describe how we fixed parameters and the
 598 procedure for Bayesian inference.

599 As explained above, context is assumed to be a discrete variable which evolves as a
 600 Markov process. The transition matrices π were generated via a Dirichlet process, with
 601 parameters that can be inferred from participant data (α and κ in Heald et al. (2021)). For
 602 a fixed value of these parameters, the transition matrices also become fixed. In our simula-
 603 tions, we set the probability of self-transitioning (denoted p_ζ) depending on the experiments
 604 (see below), to numbers that approximate the experimental setup of each study.

605 Contextual cues are assumed by the agent to be sampled from a distribution that de-
 606 pends on the current context. This is done through a set of cue probability vectors that are
 607 generated via a parametric distribution, whose parameters are fitted to participants' data.
 608 For experiments that do not include probabilistic or deceiving cues, contextual cues, when
 609 present, unequivocally reflect the current context, i.e. $p(q_t = i|c_t = j) = d_{ij}$, where d_{ij} is
 610 the Kronecker delta, equaling one when $i = j$, zero otherwise. For the simulations of Figure
 611 2, where contextual cues are probabilistic, cue uncertainty is implemented as $p(c_t = i|q_t =$
 612 $i) = 1 - \eta$, where η is the cue uncertainty, and $p(c_t = i|q_t = j) = \eta/(N_c - 1)\forall i \neq j$, where
 613 N_c is the total number of contexts in the experiment.

614 Using the above, the probability of a context for the state feedback for a trial after the
 615 cue has been observed is given by:

$$p(c_t|q_t, y_{1:t-1}) \propto p(c_t|q_t)p(c_t|c_{t-1})p(c_{t-1}|y_{1:t-1}) \quad (7)$$

616 where $p(c_t|c_{t-1})$ is given by the context self-transition (p_ζ in Table 1 below) such that:

$$p(c_t = i|c_{t-1} = j) = \begin{cases} p_\zeta & \text{if } i = j \\ \frac{1-p_\zeta}{N_c-1} & \text{otherwise} \end{cases} \quad (8)$$

617 Finally, for the hidden variables $x_{j,t}$ we chose a stationary Gaussian distribution with
 618 unknown mean μ_x and standard deviation σ_x , instead of the AR(1) a and d parameters
 619 used by Heald et al. (2021). As a consequence, the sCOIN model does not have intrinsic
 620 memory decay, instead relying on the dynamics of context inference to explain the slow
 621 decay of memories during error-clamp trials (e.g. Brennan & Smith, 2015; Scheidt et al.,
 622 2000; Vaswani & Shadmehr, 2013).

623 Using Bayesian inference, the model infers the values of μ_x and σ_x using a Gaussian
 624 likelihood and NormalGamma priors, which allowed us to use exact inference. The likelihood
 625 of the data is given by the prediction error of the observations (which drives learning):

$$p(y_t|x_t) = \mathcal{N}(y - \hat{y}, \hat{\sigma}) \quad (9)$$

626 where \hat{y} is the predicted observation given the previous observation and the previous action,
 627 and $\hat{\sigma}$ is the expected standard deviation of the predicted observation, given by the updated
 628 parameters of the model (discussed below).

629 We set priors over $\mu_{\zeta,x}$ and $\sigma_{\zeta,x}$ that enable exact inference over the latent variables x
 630 (in what follows, we dropped the j dependency for clarity):

$$\mu_x, \sigma_x \sim \mathcal{N}\mathcal{G}(\mu_0, \nu_0, \alpha_0, \beta_0) \quad (10)$$

631 with free parameters μ_0 , ν_0 , α_0 and β_0 , which we fixed for each experiment separately.
 632 Because x is context-specific, so are these parameters. This formulation comes with four
 633 free parameters (i.e. the hyper-priors $\mu_{0,i}, \nu_{0,i}, \alpha_{0,i}, \beta_{0,i}$), in accordance with the original
 634 formulation (note that Heald et al. (2021) fixed the mean of the priors for b to zero). While
 635 the two formulations are not mathematically identical, the effects of the hyper-priors for
 636 both are the same; we discuss these effects in the next section.

Because the likelihood function $p(y_t|x_t, \dots)$ is Gaussian, this choice of priors allows us to calculate the update equations as follows:

$$\begin{aligned} \mu_{\phi,i}^{(t)} &= \frac{\nu_{\phi,i}^{(t-1)} \mu_{\phi,i}^{(t-1)} + p(\zeta_i|q_t, \dots) s_t}{\nu_{\phi,t}^{(t-1)} + p(\zeta_i|q_t, \dots)} \\ \nu_{\phi,t}^{(t)} &= \nu_{\phi,t}^{(t-1)} + p(\zeta_i|q_t, \dots) \\ \alpha_{\phi,t}^{(t)} &= \alpha_{\phi,i}^{(t-1)} + p(\zeta_i|q_t, \dots)/2 \\ \beta_{\phi,i}^{(t)} &= \beta_{\phi,i}^{(t-1)} + \frac{p(\zeta_i|q_t, \dots) \nu_{\phi,i}^{(t-1)}}{\nu_{\phi,i}^{(t-1)} + p(\zeta_i|q_t, \dots)} \frac{(s_t - \mu_{\phi,t}^{(t-1)})^2}{2} \end{aligned} \quad (11)$$

637 where s_t represents the observations, in the form of the error between the observed and ex-
 638 pected outcomes of the motor command. Note that the effect of the evidence (i.e. observa-
 639 tions) on the inference over the context-dependent hidden states is gated by the probability
 640 of each context $p(\zeta_i|q_t, \dots)$, as in (Heald et al., 2021, supplementary materials).

641 **Model parameters.** Table 1 lists all the parameter values that we used during our
 642 simulations. The parameters are divided into two categories: (1) task parameters, which
 643 encode the way we simulated the experimental design; (2) agent parameters, which cor-
 644 respond to the free parameters listed in the previous section. The variable names for the
 645 model parameters are given in the “Var” column, corresponding to the variables in the
 646 previous section. The values are divided into experiments and, within experiments, into the
 647 different groups or conditions that we simulated.

648 We estimated the task parameters from the information provided in their respective
 649 publications; when direct information was not provided, we estimated it from the reported
 650 results; these estimations are not exact, but function as a proof of concept. Agent parameter
 651 values are held constant for the different conditions or groups for each experiment, except
 652 those parameters that are expected to vary across conditions.

653 Because the sCOIN model does not have a mechanism for the online creation of new
 654 contexts, relying instead of a fixed number of contexts, the number of existing contexts
 655 was set according to each experiment. For the experiments by Kim et al. (2015), to aid

	Var	Description	Kim (2015)		Oh (2019)		Davidson (2004)		Vaswani (2013)			
			Exp. 1	Exp. 2	Grp. 3A	Grp. -A	Grp. 1	Grp. 2	Grp. 3			
Task pars.	Contextual cues	Yes				No						
	x_j^*	Adaptation sizes	0, 40, -40	0, 20	0, 10	0, 4, -4	0, 4, 12	1	0, 1	-0.5, 1		
	σ_a	Adaptation noise	0.01	1		0.5		0.1				
	σ_r^*	Obs. noise	3	2.5		0.1		0.1				
Agent pars.	p_ζ	Context self-transition	0.9	0.98		0.98		0.9	0.8			
	μ_0	Hyper priors	0, -1, 1	0, 0	0, 4, -4	0, 4, 12	0, 1	0, 1, -0.5				
	ν_0		1e4, 1, 1	1e4, 1	1e4, 1, 1		1e4, 1	1e4, 1, 1				
	α_0		25e3, 0.25, 0.25	22e3, 2.2	33e3, 4e2, 4e2		5e4, 5	15e4, 5, 5				
	β_0		1e5, 2, 2	1e5, 20	1e5, 23e2, 23e2	1e5, 2	1e5, 2	1e5, 2, 2				
	σ_u	Motor noise	1	2		0.17						
	σ_r	Obs. noise	3	2.5	2.5		0.1					

Table 1

Model and simulation parameters. The star notation (e.g. x_j^*) denotes the real value used in the simulation of the task, which may be different from that assumed by the agent.

in learning of the two adaptations, the μ_0 hyperparameters were set to -1 and 1 (plus the baseline of zero), which lead to the model learning the -40 and 40 visuomotor rotation angles, respectively. As the experiments by Oh and Schweighofer (2019) have only one adaptation, this was not necessary and the new context was initiated with $\mu_0 = 0$. For the rest of the simulated experiments the focus was not on learning, but on the switching between known contexts, therefore we started simulations with models that had already learned the adaptations, setting the learned values to the real values used in each experiment.

The hyperparameters α_0 and β_0 were set first for the baseline context such that the expected standard deviation of observations β/α roughly matched the observation noise in the task, i.e. $\beta_0/\alpha_0 \sim \sigma_r + \sigma_u$, while keeping the values for β_0 and α_0 very high, which, together with the high ν_0 values, ensure that learning in this context is very slow. For the other contexts, the ratio β_0/α_0 was set to be higher than the baseline, while keeping the individual values α_0 and β_0 much lower, to speed up learning.

The exact values for α_0 and β_0 were set for each experiment such that $\beta_0/\alpha_0 = 2*(\sigma_r\sigma_a)$, where σ_a is the standard deviation of the adaptation. The rationale behind this choice is that σ_r and σ_a determine the noise in the observations made by the model at each trial, and their sum is the value of β/α to which the learning process converges with enough trials. We multiplied it by 2 in order to help in learning, specifically to make the *a priori* standard deviation higher for the untrained contexts than for the baseline context.

Of important note is the difference between the true observation noise and the expected observation noise in the simulations for the Davidson and Wolpert (2004) experiments. The expected observation noise σ_r was set to a higher value to reflect the fact that feedback in curl-force mechanical arm experiments, while devoid of any added noise, is more difficult for people to use to inform adaptation than in other types of experiments due to the nonlinear nature of the force. This fact is reflected in the high number of trials necessary for full adaptation in these experiments as compared to, for example, visuomotor rotation experiments.

683 For the simulations in Figure 2, the parameters were set as in the experiments by
 684 Davidson and Wolpert (2004), with two exceptions: (1) the cue uncertainty, which is set
 685 to the values of 0 and 0.33, for the low and high values, respectively; and (2) the agent’s
 686 observation noise σ_r , with values of 0.5 and 2.

687 **Interpreting the hyper-parameters.** μ determines the initial estimate of the adap-
 688 tation, in the same units as the necessary adaptation. ν encodes how stable this hyper-prior
 689 is: higher values (e.g. 10,000) all but guarantee that the hyper-prior μ will not change its
 690 value after observations; In principle, enough evidence should still modify it, but that would
 691 not happen during an experiment. Smaller values (i.e. ~ 1) make μ follow evidence more
 692 freely. Note that as more observations are accumulated, ν becomes bigger and bigger,
 693 stabilizing the value of μ .

694 The hyper-parameters α and β have a more complex effect. Note that the mean of a
 695 gamma distribution is β/α ; this mean is being used as the standard deviation of a Gaussian
 696 by the rest of the agent, which makes it an important measure of uncertainty. While setting
 697 the default hyper-parameters, the values used are, e.g., $\alpha = 0.5/\sigma_0$ and $\beta = 0.5$, where σ_0
 698 is the *a priori* estimate of the standard deviation of the force exerted by the environment,
 699 which controls the initial learning rate. This makes the initial standard deviation equal σ_0 ,
 700 which makes it consistent with the fixed-force model. The 0.5 values ensure that uncertainty
 701 is large at the beginning and is greatly reduced during the experiment, but never to a point
 702 where it is so small that it makes trial-to-trial variation in the environment surprising.
 703 Changing this 0.5 would make the standard deviation change more quickly, making the
 704 model more or less precise in its predictions, independently of the volatility of the mean of
 705 the adaptation (via μ).

706 The baseline model defaults to different values that make it a lot more stable. The
 707 hyper-standard deviation of the mean is set to 10,000, which makes the mean entirely
 708 stable during the duration of the experiment. The values of α and β are fixed regardless of
 709 σ_0 such that the standard deviation is 0.001 (compared that to the size of the adaptations
 710 in mechanical arm experiments, around 0.0125), and the hyper-parameters of the standard
 711 deviation are stable during the experiment.

712 Acknowledgment

713 Funded by the German Research Foundation (DFG, Deutsche Forschungsgemeinschaft)
 714 as part of Germany’s Excellence Strategy – EXC 2050/1 – Project ID 390696704 – Cluster
 715 of Excellence “Centre for Tactile Internet with Human-in-the-Loop” (CeTI) of Technische
 716 Universität Dresden.

717 References

- 718 Behrens, T. E. J., Woolrich, M. W., Walton, M. E., & Rushworth, M. F. S. (2007, September).
 719 Learning the value of information in an uncertain world. *Nature Neuroscience*, 10(9), 1214–
 720 1221. doi: 10.1038/nrn1954

- 721 Brashers-Krug, T., Shadmehr, R., & Bizzi, E. (1996, July). Consolidation in human motor memory.
722 *Nature*, 382(6588), 252–255. doi: 10.1038/382252a0
- 723 Brennan, A. E., & Smith, M. A. (2015, June). The Decay of Motor Memories Is Independent of
724 Context Change Detection. *PLoS Computational Biology*, 11(6), e1004278. doi: 10.1371/jour-
725 nal.pcbi.1004278
- 726 Criscimagna-Hemminger, S. E., & Shadmehr, R. (2008, September). Consolidation Pat-
727 terns of Human Motor Memory. *Journal of Neuroscience*, 28(39), 9610–9618. doi:
728 10.1523/JNEUROSCI.3071-08.2008
- 729 Davidson, P. R., & Wolpert, D. M. (2004, November). Scaling down motor memories:
730 De-adaptation after motor learning. *Neuroscience Letters*, 370(2-3), 102–107. doi:
731 10.1016/j.neulet.2004.08.003
- 732 Dizio, P., & Lackner, J. R. (1995, October). Motor adaptation to Coriolis force perturbations of
733 reaching movements: Endpoint but not trajectory adaptation transfers to the nonexposed
734 arm. *Journal of Neurophysiology*, 74(4), 1787–1792. doi: 10.1152/jn.1995.74.4.1787
- 735 Ernst, M. O., & Banks, M. S. (2002, January). Humans integrate visual and haptic information in
736 a statistically optimal fashion. *Nature*, 415(6870), 429–433. doi: 10.1038/415429a
- 737 Ethier, V., Zee, D. S., & Shadmehr, R. (2008, May). Spontaneous Recovery of Motor Mem-
738 ory During Saccade Adaptation. *Journal of Neurophysiology*, 99(5), 2577–2583. doi:
739 10.1152/jn.00015.2008
- 740 Forano, M., & Franklin, D. W. (2020, October). Timescales of motor memory formation in
741 dual-adaptation. *PLoS Computational Biology*, 16(10), e1008373. doi: 10.1371/jour-
742 nal.pcbi.1008373
- 743 Gandolfo, F., Mussa-Ivaldi, F. A., & Bizzi, E. (1996, April). Motor learning by field ap-
744 proximation. *Proceedings of the National Academy of Sciences*, 93(9), 3843–3846. doi:
745 10.1073/pnas.93.9.3843
- 746 Heald, J. B., Lengyel, M., & Wolpert, D. M. (2021, December). Contextual inference underlies the
747 learning of sensorimotor repertoires. *Nature*, 600(7889), 489–493. doi: 10.1038/s41586-021-
748 04129-3
- 749 Herzfeld, D. J., Kojima, Y., Soetedjo, R., & Shadmehr, R. (2018, May). Encoding of error and
750 learning to correct that error by the Purkinje cells of the cerebellum. *Nature Neuroscience*,
751 21(5), 736–743. doi: 10.1038/s41593-018-0136-y
- 752 Herzfeld, D. J., Vaswani, P. A., Marko, M. K., & Shadmehr, R. (2014, September). A memory of
753 errors in sensorimotor learning. *Science*, 345(6202), 1349–1353. doi: 10.1126/science.1253138
- 754 Howard, I. S., Ingram, J. N., Franklin, D. W., & Wolpert, D. M. (2012, September). Gone in 0.6
755 Seconds: The Encoding of Motor Memories Depends on Recent Sensorimotor States. *Journal*
756 *of Neuroscience*, 32(37), 12756–12768. doi: 10.1523/JNEUROSCI.5909-11.2012
- 757 Howard, I. S., Ingram, J. N., & Wolpert, D. M. (2010, October). Context-Dependent Partitioning
758 of Motor Learning in Bimanual Movements. *Journal of Neurophysiology*, 104(4), 2082–2091.
759 doi: 10.1152/jn.00299.2010
- 760 Huang, V. S., & Shadmehr, R. (2009, August). Persistence of Motor Memories Reflects
761 Statistics of the Learning Event. *Journal of Neurophysiology*, 102(2), 931–940. doi:
762 10.1152/jn.00237.2009
- 763 Imamizu, H., Sugimoto, N., Osu, R., Tsutsui, K., Sugiyama, K., Wada, Y., & Kawato, M. (2007,
764 August). Explicit contextual information selectively contributes to predictive switching of
765 internal models. *Experimental Brain Research*, 181(3), 395–408. doi: 10.1007/s00221-007-
766 0940-1
- 767 Kim, S., Ogawa, K., Lv, J., Schweighofer, N., & Imamizu, H. (2015, December). Neural Substrates
768 Related to Motor Memory with Multiple Timescales in Sensorimotor Adaptation. *PLoS*
769 *Biology*, 13(12), e1002312. doi: 10.1371/journal.pbio.1002312
- 770 Kojima, Y., Iwamoto, Y., & Yoshida, K. (2004, August). Memory of Learning Facilitates Sac-
771 adic Adaptation in the Monkey. *The Journal of Neuroscience*, 24(34), 7531–7539. doi:

- 772 10.1523/JNEUROSCI.1741-04.2004
773 Kording, K. P., & Wolpert, D. M. (2004, January). Bayesian integration in sensorimotor learning.
774 *Nature*, 427(6971), 244–247. doi: 10.1038/nature02169
775 Lee, J.-Y., & Schweighofer, N. (2009, August). Dual Adaptation Supports a Parallel Ar-
776 chitecture of Motor Memory. *Journal of Neuroscience*, 29(33), 10396–10404. doi:
777 10.1523/JNEUROSCI.1294-09.2009
778 Marko, M. K., Haith, A. M., Harran, M. D., & Shadmehr, R. (2012, September). Sensitivity to
779 prediction error in reach adaptation. *Journal of Neurophysiology*, 108(6), 1752–1763. doi:
780 10.1152/jn.00177.2012
781 Medina, J. F., Garcia, K. S., & Mauk, M. D. (2001, June). A Mechanism for Savings in the
782 Cerebellum. *Journal of Neuroscience*, 21(11), 4081–4089. doi: 10.1523/JNEUROSCI.21-11-
783 04081.2001
784 Nassar, M. R., McGuire, J. T., Ritz, H., & Kable, J. W. (2019, February). Dissociable Forms of
785 Uncertainty-Driven Representational Change Across the Human Brain. *Journal of Neuro-
786 science*, 39(9), 1688–1698. doi: 10.1523/JNEUROSCI.1713-18.2018
787 Oh, Y., & Schweighofer, N. (2019, November). Minimizing Precision-Weighted Sensory Prediction
788 Errors via Memory Formation and Switching in Motor Adaptation. *Journal of Neuroscience*,
789 39(46), 9237–9250. doi: 10.1523/JNEUROSCI.3250-18.2019
790 Pekny, S. E., Criscimagna-Hemminger, S. E., & Shadmehr, R. (2011, September). Protection and
791 Expression of Human Motor Memories. *The Journal of Neuroscience*, 31(39), 13829–13839.
792 doi: 10.1523/JNEUROSCI.1704-11.2011
793 Scheidt, R. A., Dingwell, J. B., & Mussa-Ivaldi, F. A. (2001, August). Learning to Move Amid
794 Uncertainty. *Journal of Neurophysiology*, 86(2), 971–985. doi: 10.1152/jn.2001.86.2.971
795 Scheidt, R. A., Reinkensmeyer, D. J., Conditt, M. A., Rymer, W. Z., & Mussa-Ivaldi, F. A. (2000,
796 August). Persistence of motor adaptation during constrained, multi-joint, arm movements.
797 *Journal of Neurophysiology*, 84(2), 853–862. doi: 10.1152/jn.2000.84.2.853
798 Scholz, J. P., & Schöner, G. (1999, May). The uncontrolled manifold concept: Identifying con-
799 trol variables for a functional task. *Experimental Brain Research*, 126(3), 289–306. doi:
800 10.1007/s002210050738
801 Shadmehr, R., & Brashers-Krug, T. (1997, January). Functional Stages in the Formation
802 of Human Long-Term Motor Memory. *Journal of Neuroscience*, 17(1), 409–419. doi:
803 10.1523/JNEUROSCI.17-01-00409.1997
804 Shadmehr, R., & Mussa-Ivaldi, F. A. (1994, May). Adaptive representation of dynamics during
805 learning of a motor task. *The Journal of Neuroscience: The Official Journal of the Society
806 for Neuroscience*, 14(5 Pt 2), 3208–3224.
807 Shmuelof, L., Huang, V. S., Haith, A. M., Delnicki, R. J., Mazzoni, P., & Krakauer, J. W. (2012, Oc-
808 tober). Overcoming Motor “Forgetting” Through Reinforcement Of Learned Actions. *Journal
809 of Neuroscience*, 32(42), 14617–14621a. doi: 10.1523/JNEUROSCI.2184-12.2012
810 Smith, M. A., Ghazizadeh, A., & Shadmehr, R. (2006, June). Interacting Adaptive Processes
811 with Different Timescales Underlie Short-Term Motor Learning. *PLoS Biology*, 4(6). doi:
812 10.1371/journal.pbio.0040179
813 Vaswani, P. A., & Shadmehr, R. (2013, May). Decay of Motor Memories in the Absence of Error.
814 *Journal of Neuroscience*, 33(18), 7700–7709. doi: 10.1523/JNEUROSCI.0124-13.2013
815 Zarahn, E., Weston, G. D., Liang, J., Mazzoni, P., & Krakauer, J. W. (2008, November). Explain-
816 ing Savings for Visuomotor Adaptation: Linear Time-Invariant State-Space Models Are Not
817 Sufficient. *Journal of Neurophysiology*, 100(5), 2537–2548. doi: 10.1152/jn.90529.2008